

Weldability of a Corrosion-Resistant Ni-Cr-Mo-Cu Alloy

Copper addition to a Ni-Cr-Mo alloy does not harm weldability, according to Vareststraint test results

M. D. ROWE, P. CROOK, AND G. L. HOBACK

ABSTRACT. Corrosion-resistant alloys based on the Ni-Cr-Mo system are used in demanding applications in chemical process, pollution control, and other industries. The ability to make sound welds in these alloys with adequate corrosion resistance is critical for their use in most applications. Vareststraint weldability testing was carried out on a Ni-Cr-Mo-Cu alloy, HASTELLOY® C-2000® (UNS N06200). Mechanical testing was conducted on weldments. Immersion corrosion tests were performed on all-weld-metal coupons of C-2000 alloy in various environments, including hydrochloric, hydrofluoric, and sulfuric acids, with other Ni-Cr-Mo alloys included for comparison. The resistance of C-2000 alloy to solidification cracking was similar to other Ni-Cr-Mo alloys that are considered to be quite weldable, including C-22® and C-276. Alloy C-2000 differs from other modern Ni-Cr-Mo alloys in that it contains 1.6 wt-% copper. Copper does not have a detrimental effect on the resistance of the alloy to solidification cracking. C-2000 alloy weld metal met the minimum tensile strength requirements of the base metal and was very ductile, passing 2 T and 1.5 T transverse bend tests. The corrosion rate of Alloy C-2000 weld metal was lower than that of the C-276 and C-22 alloys in hydrochloric, hydrofluoric, and dilute sulfuric acids, similar to that of the C-22 alloy in ASTM G28A solution, and similar to that of C-276 alloy in ASTM G28B solution and concentrated sulfuric acid.

Introduction

A Ni-Cr-Mo-Cu alloy, known commercially as HASTELLOY® C-2000® alloy (UNS N06200), was developed in the early 1990s. The alloy was designed to maximize resistance to uniform corrosion in both oxidizing and reducing acids while maintaining a high level of resistance to pitting and stress corrosion cracking in chloride environments that is typical of the Ni-Cr-Mo

alloys (Ref. 1). The modern corrosion-resistant Ni-Cr-Mo alloys have good resistance to weld metal solidification cracking. Weldability testing has been carried out previously on Ni-Cr-Mo alloys with additions of tungsten and titanium (Refs. 2, 3), but the influence of copper on weldability of the Ni-Cr-Mo alloys has not been explored in depth. Information on mechanical properties of C-2000 alloy weldments and corrosion resistance of weld metal is not available in the published literature. The solidification cracking resistance of B-3® alloy also has not been discussed in the published literature. B-3 alloy is a Ni-Mo alloy that was developed to offer improved thermal stability in comparison to B-2 alloy, while maintaining the same level of corrosion resistance in such reducing media as hydrochloric acid.

The Vareststraint weldability test is used to measure the resistance of alloys to solidification cracking. Solidification cracking occurs when partitioning of elements during solidification causes low-melting-point films to form along solidification grain boundaries. As the weld metal cools and shrinks, a level of strain may develop that exceeds the ductility of the partially solidified material and causes separation of the grain boundaries along the liquid films. This type of cracking usually appears along the weld centerline, especially in thick or heavily restrained weldments, and is present immediately after welding.

The Vareststraint test has been described in detail elsewhere (Ref. 4). In the test, a bending strain is applied to a sample while an autogenous gas tungsten arc weld is in progress. Cracking is induced in the partially solidified metal at the trailing

edge of the weld pool. The level of applied strain can be varied to tailor the severity of the test to alloys that are more or less susceptible to cracking. The amount of cracking is then quantified as the total crack length or maximum crack distance, allowing a ranking of materials with regard to cracking resistance. The minimum level of augmented strain necessary to produce cracking is another indicator of cracking susceptibility; a greater critical strain to produce cracking indicates greater resistance to cracking.

Materials and Procedure

Vareststraint Testing

The UNS numbers and trade names of the alloys are given in Table 1. The chemical compositions of alloys included in the Vareststraint test matrix are given in Tables 2 and 3. Two versions of the Vareststraint test were used: the full-scale and subscale Vareststraint tests. Vareststraint welding parameters are given in Table 4. A larger weld bead is produced in the full-scale test, resulting in longer and more numerous cracks, which are easier to count and measure. The subscale test is more economical than the full-scale test, allowing for a greater number of alloys to be tested and a greater number of replicate tests for improved statistical significance of results. Testing was performed in triplicate unless otherwise noted. After testing, the specimens were lightly buffed with a fine non-woven abrasive to remove any surface oxide, then the cracks were measured under a stereo zoom microscope equipped with a filar eyepiece. Crack length was measured as the perpendicular distance from the location of the solid-liquid interface at the time of loading. Both the total crack length (TCL) and the maximum crack distance (MCD) were reported. The MCD, along with the temperature gradient adjacent to the weld pool, can be taken as an indicator of the brittle temperature range (BTR) for a given alloy (Ref. 5). In the present investigation, it can be assumed that for a given set of welding parameters and similar material

KEY WORDS

Corrosion Resistance
Nickel-Based Alloys
HASTELLOY® C-2000®
Vareststraint Test
Solidification Cracking

M. D. ROWE, P. CROOK, and G. L. HOBACK
are with Haynes International Inc., Kokomo, Ind.

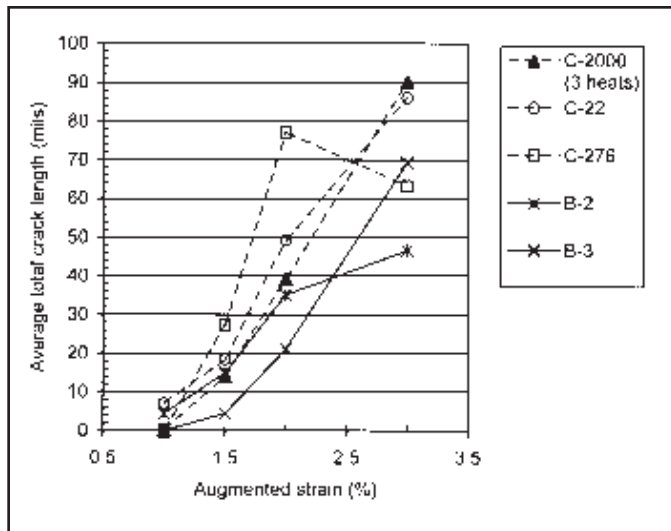


Fig. 1 — Full-scale Varestraint test results. Average total crack length vs. percent augmented strain.

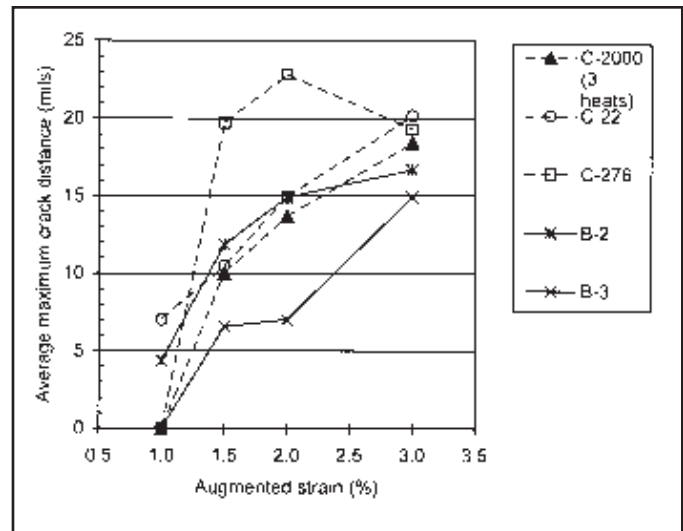


Fig. 2 — Full-scale Varestraint test results. Average maximum crack distance vs. percent augmented strain.

properties, the MCD gives an indication of the temperature range over which a given alloy is susceptible to solidification cracking.

Table 1 — UNS Numbers and Trade Names of Alloys

UNS No.	Trade Name
N10276	HASTELLOY ^{®(a)} C-276
N06022	HASTELLOY C-22 [®]
N06200	HASTELLOY C-2000 [®]
N06059	NICROFER ^{®(b)} 5923 hMo (Alloy 59)
N06686	INCONEL ^{®(c)} 686
N10665	HASTELLOY B-2
N10675	HASTELLOY B-3 [®]
N06625	HAYNES [®] 625

(a) HASTELLOY, HAYNES, C-22, C-2000, and B-3 are trademarks of Haynes International, Inc.

(b) NICROFER is a trademark of Krupp-VDM GmbH.

(c) INCONEL is a trademark of the Special Metals group of companies.

Measurement of Elemental Partitioning in Weld Metal

One metallographic mount, in plan view, was prepared from a representative full-scale test specimen of each alloy at the location of the solid-liquid interface at the time of loading. Locations were identified on the etched surface where the cellular solidification structure was running parallel to the surface of the sample. These locations were marked with microhardness indentations, then the sample was repolished. Both energy-dispersive (EDS) and wavelength-dispersive (WDS) X-ray spectroscopy measurements were made in the scanning electron microscope to quantify the partitioning of alloying elements.

A useful way to quantify the tendency of a given alloying element to segregate during solidification is with the equilibrium partition coefficient (k). Microscopic segregation in weld metal can be described using the Scheil equation, which

gives the composition of the first solid to form (at the dendrite core) as the nominal alloy composition multiplied by the partition coefficient, k . If the value of k for a given alloying element is less than unity, the dendrite core will be depleted in that element, as is the case for molybdenum in nickel-based alloys.

It is possible to approximate k for a given element in an alloy by dividing the measured dendrite core composition by the bulk alloy composition (Ref. 6). Four representative alloys were selected for EDS analysis of microsegregation. Additional WDS measurements were made on Alloy C-2000. When calculating k , the bulk alloy composition was measured by an area scan of the weld metal for EDS, and several spot measurements in the wrought base metal for WDS. By using the same technique to measure both the dendrite core and the nominal compositions for a given calculation of k , it was expected that the influence of systematic error in a

Table 2 — Chemical Composition of Alloys Evaluated with the Full-Scale Varestraint Test (wt-%)

Alloy Heat No.	C-276 2760-9-3740	C-22 2277-7-3179	C-2000 2316-9-8046	C-2000 2316-6-8006	C-2000 2316-6-8007	B-2 2665-9-6284	B-3 2675-9-6678
C	0.0027	0.0027	0.0041	0.0025	0.0041	0.003	0.002
Nb	0.25	<0.05	<0.05	0.01	<0.05	<0.10	<0.05
Co	0.97	1.03	0.15	0.04	<0.05	<0.10	<0.10
Cr	15.85	21.52	22.60	22.15	22.92	0.82	1.81
Cu	0.10	0.05	1.65	1.46	1.51	0.05	0.02
Fe	6.45	4.73	0.52	0.69	0.74	1.67	1.87
Mn	0.49	0.24	0.23	0.19	0.23	0.82	0.56
Mo	15.56	13.41	15.57	15.94	16.54	27.89	27.99
Ni	55.75	55.61	58.3	59.07	57.85	69.4	66.33
P	0.008	0.007	0.003	0.005	0.005	<0.010	<0.004
S	0.0013	0.0016	0.0026	0.0018	0.0026	0.003	0.003
Si	0.02	0.027	0.034	0.01	<0.020	0.04	<0.02
Ti	<0.01	<0.01	<0.05	<0.01	<0.05	—	<0.01
V	0.17	0.13	<0.05	0.01	<0.05	<0.01	<0.01
W	3.52	3.03	0.10	0.10	0.12	<0.10	0.93

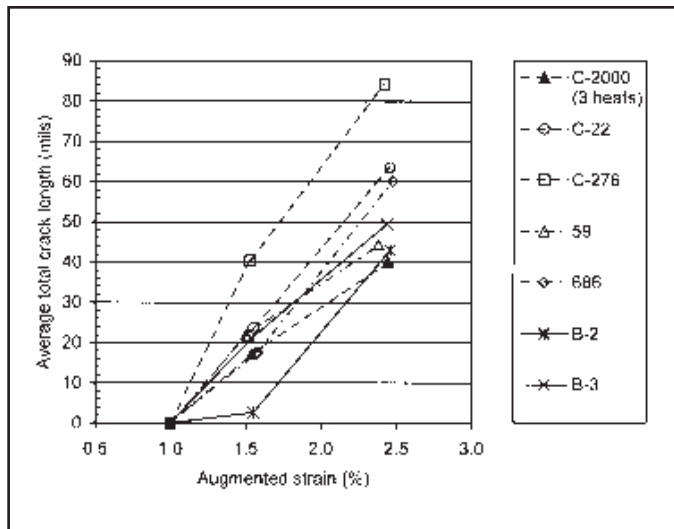


Fig. 3 — Subscale Varestraint test results. Average total crack length vs. percent augmented strain.

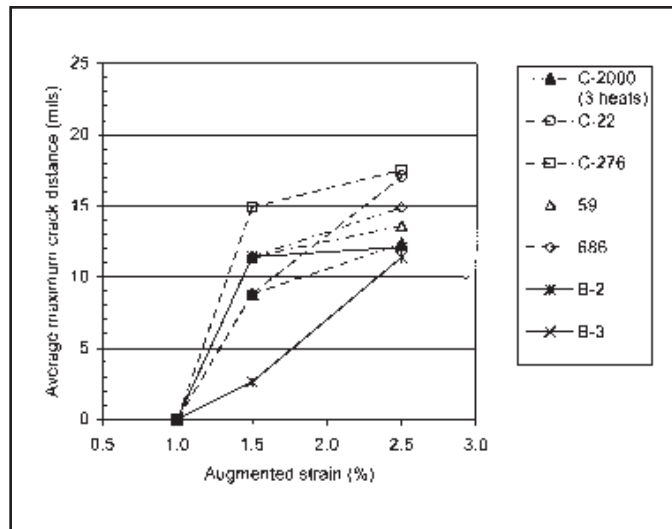


Fig. 4 — Subscale Varestraint test results. Average maximum crack distance vs. percent augmented strain.

Table 3 — Chemical Composition of Alloys Evaluated with the Subscale Varestraint Test (wt-%)

Alloy Heat No.	C-276 2760-8-3657	C-22 2277-8-3159	C-2000 2316-4-8000	C-2000 2316-9-8024	C-2000 2316-6-8005	59 45241	686 NX19-01BK	B-2 2665-8-6273	B-3 2675-4-6656	625 2650-6-6993
C	0.0031	0.0030	0.0020	0.0038	0.0030	0.0053	0.0042	0.0030	0.0020	0.02
Nb	0.05	0.05	0.03	0.05	0.01	<0.05	<0.05	<0.10	<0.01	3.65
Co	1.53	0.85	0.01	0.10	0.03	<0.05	<0.05	<0.10	0.02	0.17
Cr	15.55	21.82	23.11	22.61	22.78	22.58	20.36	0.74	1.43	21.55
Cu	0.07	0.09	1.68	1.59	1.57	0.03	0.03	0.01	0.01	0.04
Fe	5.99	4.01	0.25	1.17	0.68	0.55	0.21	1.69	1.48	4.40
Mn	0.50	0.20	0.20	0.22	0.22	0.17	0.25	0.75	0.64	0.27
Mo	15.41	13.32	16.23	15.74	15.89	15.97	16.20	28.03	27.81	9.07
Ni	55.34	56.47	57.79	57.55	58.00	60.26	59.15	65.94	67.69	59.27
P	0.007	0.006	<0.004	0.003	0.003	0.003	0.003	<0.004	0.004	0.006
S	0.0014	0.0035	0.0040	0.0030	0.0060	0.0013	0.0015	0.0020	0.0030	0.002
Si	0.04	0.03	0.02	0.02	0.01	0.05	0.038	0.02	0.01	0.17
Ti	0.01	0.01	<0.01	0.05	<0.01	<0.05	0.07	—	<0.01	0.25
V	0.15	0.18	<0.01	0.05	<0.01	0.13	<0.05	<0.01	0.01	—
W	3.98	2.84	0.06	0.05	0.09	<0.05	3.94	<0.01	0.04	0.11

given measurement technique would be minimized. To give an estimate of the uncertainty in the analysis, k was calculated from at least five independent dendrite core measurements. The mean and 95% confidence limits were calculated from the five replicate measurements of k . In the calculation of k , no attempt was made to correct for solid-state diffusion during cooling of the weld to room temperature.

Mechanical Testing

Plate weldments were prepared for mechanical testing using C-2000 alloy plate, 1 to 1.5 in. (25 to 38 mm) thick. Matching composition filler metal was used. A single V-groove weld preparation with a 70-deg included angle and 0.125-in. (3.2-mm) root opening was used for transverse tensile testing. All-weld-metal tensile and Charpy specimens were taken

Table 4 — Varestraint Welding Parameters

	Full Scale	Subscale
Specimen dimensions, in. (mm)	2 x 12 x 0.375 (51 x 305 x 10)	1 x 6 x 0.125 (25 x 152 x 3)
Current (A)	220	70
Travel speed, in./min (mm/s)	4.5 (1.9)	4.5 (1.9)
Arc length, in. (mm)	0.094 (2.4)	0.037 (0.94)
Shielding gas, ft ³ /h (L/s), argon	35 (0.28)	35 (0.28)
Tungsten electrode type	2% Thoriated	2% Thoriated
Tungsten electrode diameter, in. (mm)	0.125 (3.2)	0.094 (2.4)
Electrode included angle (degree)	60	60

from a 1-in.-thick plate using a 20-deg included angle, single-sided preparation with a 0.75-in. (19-mm) root opening and matching composition backing bar. All welding was performed manually in the flat position. Welding parameters are given in Table 5. All-weld-metal tensile testing was performed according to Euro-

pean Standard EN 876. The specimen was a round bar with a 0.394-in. (10-mm) diameter by 1.97-in. (50-mm) gauge length. Transverse tensile testing was performed according to European Standard EN 895. Specimens had a rectangular cross section measuring 1.00 x 0.67 in. (25 x 17 mm) and a 3.35-in. (85-mm) gauge length. The av-

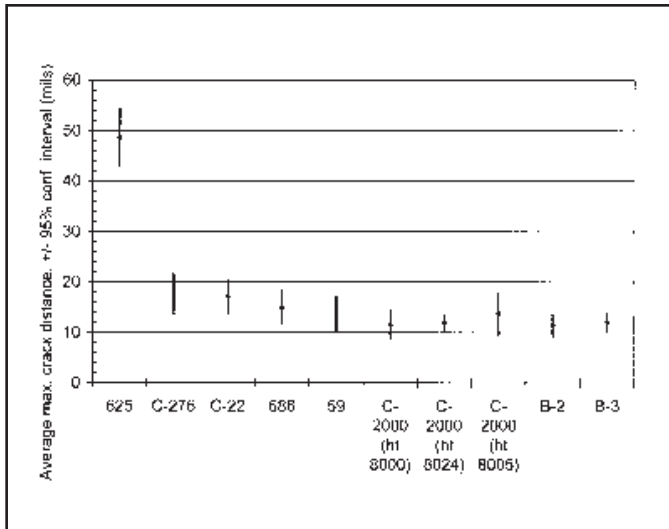


Fig. 5 — Subscale V restraint test results. Comparison of average maximum crack distance for various alloys at 2.5% augmented strain, showing experimental error.

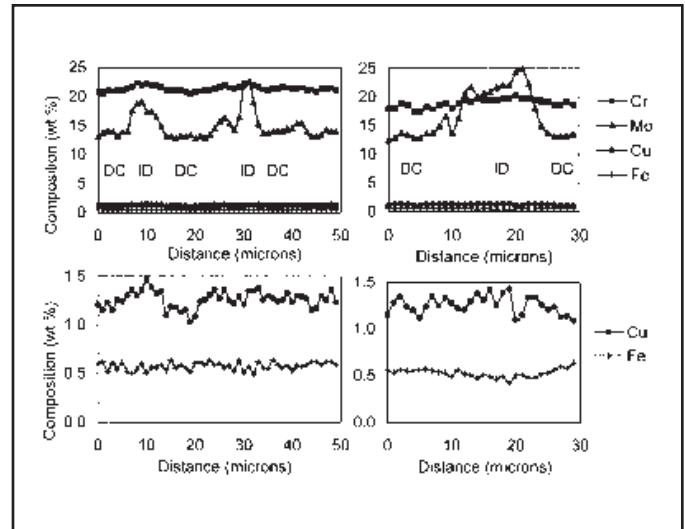


Fig. 6 — WDS compositional measurements of microsegregation in the weld metal of C-2000 alloy. "DC" indicates dendrite core locations. "ID" indicates interdendritic locations. The two lower plots show the same data as the upper plots only on a smaller scale.

Table 5 — Welding Parameters for Weldments Subjected to Mechanical Testing

Test specimens removed from plate	Welding process	Shielding gas	Current (A)	Arc voltage (V)	Filler metal diameter, in. (mm)	Number of passes	Plate thickness, in. (mm)
AWM tensile, Charpy	GTAW	100% Ar	190–240	12–14	0.094 (2.4), 0.125 (3.2)	31	1 (25)
Transv. tensile	GTAW	100% Ar	140–230	12–14	0.094 (2.4), 0.125 (3.2)	32	1 (25)
AWM tensile, Charpy	GMAW-pulse	75% Ar-25% He	180	28–30	0.045 (1.1)	22	1 (25)
Transv. tensile	GMAW-pulse	75% Ar-25% He	175	28–30	0.045 (1.1)	55	1.5 (38)
AWM tensile, Charpy	SMAW	none	95–135	23–24	0.125 (3.2), 0.156 (4.0)	43	1 (25)
Transv. tensile	SMAW	none	95–135	23–24	0.125 (3.2), 0.156 (4.0)	29	1 (25)

erage of two replicate tensile tests was reported. Charpy impact toughness testing was performed according to the ASTM E23 specification using full-sized bars. The notch was oriented vertically through the weld centerline. The average of three replicate Charpy impact tests was reported.

Weld Metal Corrosion Testing

Half-inch (13-mm) -diameter bars were removed from an undiluted GTAW weld metal buildup. The bars were then sectioned into 0.25-in. (6.4-mm) -thick cylindrical slices for corrosion testing. Immersion corrosion tests were performed in flasks equipped with condensers to control evaporation. No special efforts were made to aerate or deaerate the solution. The ASTM G28A and G28B tests were not designed for use on weld metal, but these solutions do provide very severe test environments for ranking of alloys.

Results and Discussion

Varestraint results are given in Tables 6 and 7. The average values for full-scale and subscale tests are plotted in Figs. 1–4. Inspection of the data reveals that the experimental uncertainty is similar in magnitude to the differences between alloys in many cases; therefore, the alloy ranking varies somewhat from one data set to another in Figs. 1–4. In most cases, the Ni-Mo alloys are slightly less susceptible to solidification cracking than the Ni-Cr-Mo alloys according to the average values. Alloy C-276 appears to be slightly more susceptible to solidification cracking than the high-chromium Ni-Cr-Mo alloys. This ranking is similar to prior work, which indicated that C-276 alloy is slightly more susceptible than C-22 alloy (Ref. 2) and that C-276 is slightly more susceptible than 59 alloy (Ref. 3). The MCD results, plotted in Fig. 5, allow for a comparison between alloys taking into account the ex-

perimental uncertainty. This data set is based on six replicate tests per alloy, giving slightly better statistical confidence than the other data sets, which were based on three replicate tests. Alloy 625, containing niobium, is more susceptible to solidification cracking than the niobium-free alloys. This observation is consistent with prior work (Ref. 3). All of the niobium-free alloys were similar in their resistance to solidification cracking and have a history of good weldability in industry. The TCL measurement parameter produced a similar ranking.

Niobium in 625 alloy has a strong tendency to partition to the liquid and forms a relatively low-melting terminal solidification product containing NbC and/or Laves phase (Refs. 7, 8). The niobium-free Ni-Cr-Mo alloys form a terminal solidification product containing the topologically close-packed (TCP) phases sigma, P, or mu (Ref. 2), which is less detrimental to weldability than the Nb-rich Laves phase.

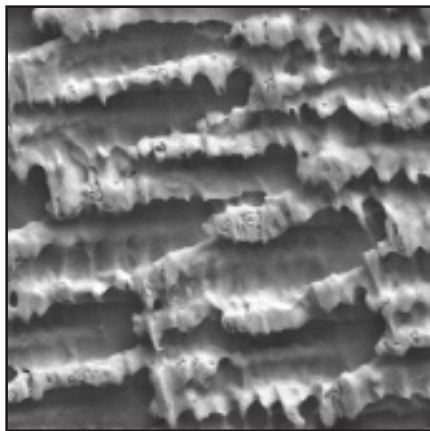
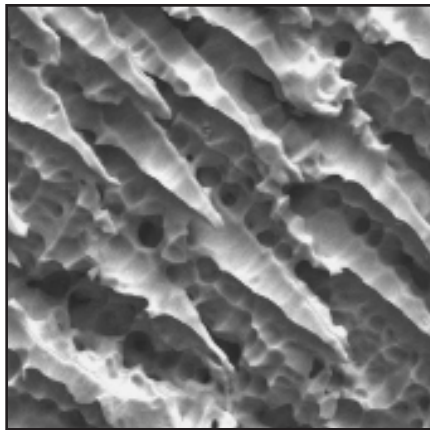


Fig. 7 — SEM secondary electron images of corroded surfaces of C-2000 alloy all-weld-metal corrosion test specimens. Nitric acid attacked the interdendritic areas (top), while hydrochloric acid attacked the dendrite cores (bottom).

Alloy C-2000 differs from the other Ni-Cr-Mo alloys in that it contains copper. The Varestraint test results indicate that the addition of copper does not have any detrimental effect on weldability. The weldability of B-3 alloy also does not differ significantly from the other Nb-free Ni-Cr-Mo and Ni-Mo alloys.

Mechanical Testing

The Varestraint test is useful for providing a relative ranking between alloys, but actual weldments are more appropriate to determine if an alloy is weldable under realistic fabrication conditions. Heavy plate weldments were produced using various welding processes and subjected to mechanical testing. Mechanical test results are given in Tables 8–10. All-weld-metal and transverse tensile tests gave values in excess of the 100 ksi minimum ultimate tensile strength specified for wrought C-2000 alloy plate. Weld metal showed substantial ductility and failure typically occurred in the base metal for transverse tests. Substantial Charpy impact toughness is maintained from room

Table 6 — Full-Scale Varestraint Test Results

Alloy	Heat No.	Strain (%)							
		1.0		1.5		2.0		3.0	
		TCL, mils (mm)	±	TCL, mils (mm)	±	TCL, mils (mm)	±	TCL, mils (mm)	±
C-276	2760-9-3740	0	0	27 (0.7)	90	77 (2.0)	65	63 (1.6)	20
C-22	2277-7-3179	7 (0.2)	16	18 (0.5)	40	49 (1.2)	8	86 (2.2)	64
C-2000	2316-9-8046	0	0	13 (0.3)	57	50 (1.3)	45	81 (2.1)	57
C-2000	2316-6-8006	0	0	0	0	15 (0.4)	36	77 (2.0)	59
C-2000	2316-6-8007	0	0	29 (0.7)	74	53 (1.3)	39	112 (2.8)	31
C-2000	avg. 3 heats	0	0	14 (0.4)	17	39 (1.0)	18	90 (2.3)	19
B-2	2665-9-6284	4 (0.1)	19	15 (0.4)	34	35 (0.9)	15	46 (1.2)	61
B-3	2675-9-6678	0	0	4 (0.1)	19	21 (0.5)	52	69 (1.8)	29

Alloy	Heat No.	Strain (%)							
		1.0		1.5		2.0		3.0	
		MCD, mils (mm)	±	MCD, mils (mm)	±	MCD, mils (mm)	±	MCD, mils (mm)	±
C-276	2760-9-3740	0	0	20 (0.5)	9	23 (0.6)	4	19 (0.5)	7
C-22	2277-7-3179	7 (0.2)	7	11 (0.3)	9	15 (0.4)	2	20 (0.6)	4
C-2000	2316-9-8046	0	0	8 (0.2)	11	14 (0.4)	2	17 (0.4)	2
C-2000	2316-6-8006	0	0	0	0	10 (0.3)	8	16 (0.4)	3
C-2000	2316-6-8007	0	0	15 (0.4)	7	18 (0.5)	2	22 (0.6)	4
C-2000	avg. 3 heats	0	0	10 (0.3)	9	14 (0.4)	4	18 (0.5)	3
B-2	2665-9-6284	4 (0.1)	8	12 (0.3)	2	15 (0.4)	4	17 (0.4)	4
B-3	2675-9-6678	0	0	7 (0.2)	9	7 (0.2)	6	15 (0.4)	3

Notes: TCL is average Total Crack Length; MCD is average Maximum Crack Distance. Values are average of three replicate tests. ± 95% confidence interval on the mean in mils.

Table 7 — Subscale Varestraint Test Results

Alloy	Heat No.	Strain (%)					
		1.0		1.5		2.5	
		TCL, mils (mm)	±	TCL, mils (mm)	±	TCL, mils (mm)	±
C-276	2760-8-3657	0	0	40 (1.0)	19	84 (2.1)	20
C-22	2277-8-3159	0	0	24 (0.6)	41	64 (1.6)	27
C-2000	2316-4-8000	0	0	22 (0.6)	19	29 (0.7)	22
C-2000	2316-9-8024	0	0	6 (0.2)	14	44 (1.1)	27
C-2000	2316-6-8005	0	0	24 (0.6)	17	46 (1.2)	30
C-2000	avg. 3 heats	0	0	17 (0.4)	8	40 (1.0)	13
59	45241	0	0	22 (0.6)	4	44 (1.1)	4
686	NX1901BK	0	0	18 (0.5)	26	60 (1.5)	17
B-2	2665-8-6273	0	0	3 (0.1)	11	43 (1.1)	13
B-3	2675-4-6656	0	0	21 (0.5)	17	49 (1.2)	20
625	2650-6-6993	67 (1.7)	31	188 (4.8)	25	269 (6.8)	77

Alloy	Heat No.	Strain (%)					
		1.0		1.5		2.5	
		MCD, mils (mm)	±	MCD, mils (mm)	±	MCD, mils (mm)	±
C-276	2760-8-3657	0	0	15 (0.4)	10	18 (0.5)	4
C-22	2277-8-3159	0	0	9 (0.2)	10	17 (0.4)	3
C-2000	2316-4-8000	0	0	10 (0.3)	4	12 (0.3)	3
C-2000	2316-9-8024	0	0	6 (0.2)	14	12 (0.3)	2
C-2000	2316-6-8005	0	0	11 (0.3)	0	14 (0.4)	4
C-2000	avg. 3 heats	0	0	9 (0.2)	3	12 (0.3)	1
59	45241	0	0	11 (0.3)	8	14 (0.4)	4
686	NX1901BK	0	0	11 (0.3)	8	15 (0.4)	3
B-2	2665-8-6273	0	0	3 (0.1)	11	11 (0.3)	2
B-3	2675-4-6656	0	0	11 (0.3)	4	12 (0.3)	2
625	2650-6-6993	24 (0.6)	7	43 (1.1)	15	49 (1.2)	6

Notes: TCL is average Total Crack Length; MCD is average Maximum Crack Distance. Values are average of six tests for subscale, 2.5% strain. Average of three for all others. ± 95% confidence interval on the mean in mils.

Table 8 — All-Weld-Metal Tensile Test Results

Welding process	UTS, ksi (MPa)	Std. dev. (ksi)	0.2% Yield, ksi (MPa)	Std. dev. (ksi)	Elongation (%)	Std. dev.	Reduction of area (%)	Std. dev.
GTAW	108 (744)	3	75 (517)	1	40	5	48	2
GMAW	109 (752)	4	73 (503)	3	40	5	44	2
SMAW	108 (744)	0	73 (503)	0	42	5	40	6

Table 9 — Transverse Weldment Tensile Test Results

Welding process	UTS, ksi (MPa)	Std. dev. (ksi)	0.2% Yield, ksi (MPa)	Std. dev. (ksi)	Elongation (%)	Std. dev.	Failure location
GTAW	104 (717)	0	59 (407)	0	56	1	Base metal
GMAW	107 (738)	4	60 (414)	2	55	3	Base metal
SMAW	104 (717)	1	53 (365)	4	58	0	Base metal

Table 10 — Charpy V-Notch Impact Toughness Test Results, ft-lb (J)

Welding process	Notch location	Room temp.	Std. dev., ft-lb	-184°F (-120°C)	Std. dev., ft-lb	-320°F (-196°C)	Std. dev., ft-lb
GTAW	Weld metal	111 (151)	6	89 (121)	10	79 (107)	7
GMAW	Weld metal	92 (125)	8	86 (117)	4	68 (92)	5
SMAW	Weld metal	50 (68)	2	44 (60)	2	36 (49)	1
All	HAZ	—	—	—	—	>263 (>357)	—

temperature to cryogenic temperatures in the as-welded condition, which is typical of Ni-Cr-Mo alloys. Ductility and impact toughness of the weld metal, while high compared to many structural materials, is somewhat less than that of the wrought alloy. This may be due to the formation of an interdendritic TCP phase constituent in the weld metal upon solidification. Other Ni-Cr-Mo corrosion-resistant alloys have been shown to contain TCP phases in the terminal solidification product (Ref. 2). The impact toughness of weld metal deposited by shielded metal arc welding (SMAW) is less than that of weld metal deposited by the inert gas processes gas tungsten arc welding (GTAW) and gas metal arc welding (GMAW). This trend is also typical of nickel-based alloys and austenitic stainless steels in general. Higher weld metal oxygen content, and thus greater content of oxide inclusions, produced by flux-bearing processes causes a reduction in impact toughness. The impact toughness of weld metal deposited by

Table 11 — SEM-EDS Compositional Measurements of Partitioning in Weld Metal from Representative Full-Scale Vastrestraint Specimens

Alloy	Heat No.		Cr	Co	Mn	Fe	Ni	Cu	Mo	W
C-2000	2316-9-8046	Base	22.37	—	0.44	0.53	58.44	2.13	15.76	—
		Backfill	22.52	—	0.50	0.68	52.53	2.15	21.61	—
		Core	22.13	—	0.39	0.69	60.98	2.06	13.74	—
B-3	2675-9-6678	Base	2.08	—	0.47	1.99	66.29	—	28.75	—
		Backfill	1.89	—	1.20	1.73	54.83	—	40.36	—
		Core	2.16	—	0.64	2.02	69.84	—	24.84	—
C-22	2277-7-3179	Base	21.51	1.07	—	5.07	55.25	—	13.34	3.76
		Backfill	22.08	1.35	—	4.54	46.25	—	21.15	4.28
		Core	21.82	0.96	—	5.18	56.77	—	11.11	4.17
C-276	2760-9-3740	Base	16.28	1.04	—	6.76	56.22	—	16.32	2.76
		Backfill	18.81	0.61	—	5.70	46.38	—	23.85	4.65
		Core	16.38	0.97	—	7.04	58.45	—	11.94	5.22

Notes: All values are in weight percent, and represent single measurements.

Base: wrought base metal composition by EDS.

Core: dendrite core composition by EDS.

Backfill: composition of the terminal solidification product in a backfilled crack by EDS.

Table 12 — Calculated Values of the Distribution Coefficient (*k*)

Alloy	Method	Cr	±	Fe	±	Ni	±	Cu	±	Mo	±	W	±
C-2000	EDS	1.02	0.02	—	—	1.05	0.01	0.82	0.04	0.85	0.03	—	—
C-2000	WDS	0.96	0.04	1.06	0.10	1.02	0.03	0.89	0.11	0.91	0.03	—	—
B-2	EDS	—	—	—	—	1.04	0.01	—	—	0.90	0.03	—	—
B-3	EDS	—	—	—	—	1.03	0.01	—	—	0.89	0.04	—	—
C-22	EDS	1.00	0.05	1.06	0.05	1.04	0.02	—	—	0.82	0.05	0.97	0.14
C-276	EDS	1.01	0.04	1.07	0.04	1.04	0.02	—	—	0.86	0.03	0.80	0.12

SMAW is sufficient for most applications, but if maximum impact toughness is desired, an inert gas welding process is recommended. The weldments also passed 2 T and 1.5 T side bend tests, indicating good ductility and sound weld metal. No evidence of solidification cracking was encountered in the plate weldment trials.

Elemental Partitioning in Weld Metal

Results of elemental partitioning measurements from various locations in the weld metal can be seen in Table 11. The “backfill” regions mentioned in Table 11 are locations where cracks induced by Vareststraint testing drew in some of the terminal solidification product. The back-filled regions are a convenient location to measure the composition of the terminal solidification product. The most apparent trend is depletion of the dendrite cores in molybdenum and consequent enrichment of the interdendritic areas. For many highly alloyed nickel-based materials, the remaining liquid becomes increasingly enriched in alloying elements such as molybdenum as solidification proceeds until a composition is reached where solidification terminates by formation of a TCP phase (Ref. 9).

Values of the distribution coefficient (*k*) calculated from EDS measurements are given in Table 12. The measurements on C-2000 alloy were also confirmed using WDS. Those values that have an uncertainty of less than about ±0.05 compare favorably with reported values from the published literature, which are summarized in Table 13. There is some uncertainty in the measured *k* values of tungsten due to the low nominal alloy content, but this element is expected to behave in a similar manner to molybdenum, as indicated in Table 13 (Ref. 10).

The *k* value for copper in C-2000 alloy indicates that copper has a slight tendency to segregate to the terminal solidification product; however, the overall variation in copper content is small due to the low nominal content of copper in the alloy. The partitioning of alloying elements in

Table 13 — Values of the Distribution Coefficient (*k*) Reported in the Literature for Various Nickel- and Iron-Based Alloys

Ref.	Alloy	Cr	Fe	Ni	Nb	Mo	W
10	230	1.02	1.56	0.97	—	—	0.85
11	718	1.03	1.04	1.00	0.48	—	—
11	909	—	1.10	0.97	0.49	0.82	—
12	242	1.00	—	1.04	—	0.88	—
13	718	1.02	1.06	—	0.48	0.87	—
7	625	—	—	—	0.54	—	—
8	Ni-base 625 type	1.06	1.00	1.02	0.45	—	—
8	Fe-base 625 type	1.02	1.06	1.00	0.25	—	—
8	625 overlay on steel	1.05	1.02	1.04	0.46	—	—
8	20Cb-3	0.96	1.08	0.97	0.33	—	—

C-2000 alloy weld metal is shown in Fig. 6. The dendrite cores can be expected to have a copper content that is 80 to 90% of the nominal alloy composition, and the interdendritic regions will be somewhat enriched in copper.

Corrosion Testing of Weld Metal

Results of immersion corrosion tests on all-weld-metal specimens of Ni-Cr-Mo alloys are given in Table 14. Even though these alloys have similar chemical compositions, each displayed advantages in certain environments. The high chromium alloys, C-22, C-2000, and 59, performed well in the oxidizing test environments, ASTM G28A, and boiling nitric acid. In the severe pitting corrosion test environment described in ASTM G28B, Alloys 59 and 686 resisted pitting, while the other alloys showed some degree of pitting corrosion. Alloy C-2000 showed the lowest corrosion rates in hydrochloric and hydrofluoric acid test environments. In concentrated sulfuric acid, the high-molybdenum alloys containing either tungsten or copper — C-276, C-2000, and 686 — gave low corrosion rates.

Weld metal is typically more susceptible to corrosion than wrought material of the matching composition due to elemental partitioning during solidification. SEM secondary electron images of C-2000 alloy weld metal corrosion test specimens are shown in Fig. 7, illustrating the influence of compositional variations on corrosion

behavior. In nitric acid, chromium is the primary beneficial alloying element and high concentrations of molybdenum can be detrimental; therefore, preferential corrosion occurred at the interdendritic locations where the molybdenum concentration is elevated, as indicated in Fig. 6. The opposite corrosion morphology occurred in hydrochloric acid, where molybdenum and copper are the beneficial alloying elements; preferential corrosion occurred at the dendrite cores.

The detrimental influence of elemental partitioning on corrosion performance is a problem common to all molybdenum-bearing nickel-based alloys and stainless steels. In the case of molybdenum-bearing stainless steels, an overalloyed filler metal with a higher nominal molybdenum content is sometimes selected to mitigate the problem. However, localized corrosion can still occur in the unmixed zone adjacent to the fusion boundary (Ref. 14). Overalloyed filler metals are typically not available for the highly alloyed Ni-Cr-Mo alloys due to the fact that a higher overall alloy content tends to promote formation of harmful intermetallic phases. The corrosion test results listed in Table 14 indicate that certain filler metals outperform others in specific corrosive environments, but no one alloy qualifies as an overalloyed filler metal throughout the entire range of corrosive environments. Therefore, dissimilar filler metals may be used to join the corrosion-resistant nickel-based alloys in special cases where a spe-

Table 14 — Immersion Corrosion Test Results for All-Weld-Metal Specimens, mpy (mm/y)

Environment	Temp., °F (°C)	C-22	C-276	C-2000	59	686
ASTM G28A	Boiling	31.4 (0.80)	274 (6.96)	32.2 (0.82)	31.8 (0.81)	105 (2.67)
ASTM G28B	Boiling	P/P	P/NP	P/NP	NP/NP	NP/NP
65% HNO ₃	Boiling	74.5 (1.89)	734 (18.6)	88.1 (2.24)	85.3 (2.17)	394 (10.0)
2.5% HCl	175 (79)	15.5 (0.39)	4.1 (0.10)	0.1 (0.003)	0.1 (0.003)	0.1 (0.003)
5% HCl	175 (79)	102.4 (2.60)	47.9 (1.21)	0.2 (0.005)	22 (0.56)	31.7 (0.81)
20% HF	175 (79)	151.5 (3.85)	46.1 (1.17)	22.9 (0.58)	132 (3.35)	41.6 (1.06)
48% HF	175 (79)	636.5 (16.2)	54.5 (1.38)	26.3 (0.67)	326 (8.28)	239.5 (6.08)
70% H ₂ SO ₄	175 (79)	29.3 (0.74)	11.3 (0.29)	10.1 (0.26)	29.6 (0.75)	9.4 (0.24)

Notes: G28A is 50% sulfuric acid + ferric sulfate; G28B is 23% sulfuric acid + 1.2% hydrochloric acid + 1% ferric chloride + 1% cupric chloride. Results are average of duplicate tests. For G28B test, results of the two tests are given individually: P indicates the sample pitted, NP indicates the sample did not pit.

cific problem has been identified, but, for general use, matching composition filler metals are recommended to take advantage of the special characteristics of each alloy.

Conclusions

1) Vareststraint testing indicated that C-2000 alloy containing copper and the Ni-Mo alloy B-3 exhibit resistance to solidification cracking that is similar to other corrosion-resistant Ni-Cr-Mo and Ni-Mo alloys that have a history of good weldability in industry. The niobium-free Ni-Cr-Mo and Ni-Mo alloys tested were more resistant to solidification cracking than the niobium-containing Alloy 625.

2) Heavy plate weldments using C-2000 alloy plate and matching composition filler metal showed no indication of solidification cracking. Ultimate tensile strength of weldments exceeded the 100-ksi minimum specified tensile strength of the wrought alloy.

3) Modern Ni-Cr-Mo alloy filler metals each show advantages in certain corrosive environments. Matching filler metals should be used to join these alloys in most applications to take advantage of the special characteristics of each alloy.

References

1. Crook, P., Caruso, M. L., and Kingseed,

D. A. 1997. Corrosion resistance of a new, wrought Ni-Cr-Mo alloy. *Materials Performance* 36(3): 49-52.

2. Cieslack, M. J., Headley, T. J., and Romig, Jr., A. D. 1986. The welding metallurgy of HASTELLOY alloys C-4, C-22, and C-276. *Metallurgical Transactions A* 17A(11): 2035-2047.

3. Brill, U., Hoffman, T., and Wilken, K. 1990. Solidification cracking: Super stainless steels and nickel-base alloys. *Proceedings of the Weldability of Materials: Materials Weldability Symposium*, 99-105. Materials Park, Ohio: ASM International.

4. Savage, W. F., and Lundin, C. D. 1965. The Vareststraint test. *Welding Journal* 44(10): 433-s to 442-s.

5. Matsuda, F., Nakagawa, H., Katayama, S., and Arata, Y. 1982. Weld metal cracking and improvement of 25%Cr-20%Ni (AISI 310S) fully austenitic stainless steel. *Transactions of the Japan Welding Institute* 13(2): 41-58.

6. DuPont, J. N., Micheal, J. R., and Newbury, B. D. 1999. Welding metallurgy of Alloy HR-160®. *Welding Journal* 78(12): 408-s to 415-s.

7. Cieslack, M. J., Headley, T. J., Kollie, T., and Romig, A. D. 1988. A melting and solidification study of Alloy 625. *Metallurgical Transactions* 19A(9): 2319-2331.

8. DuPont, J. N., Robino, C. V., Marder, A. R., and Notis, M. R. 1998. Solidification of Nb-bearing superalloys: Part II — Pseudoternary solidification surfaces. *Metallurgical Transactions* 29A(11): 2797-2806.

9. Cieslack, M. J., Knorovsky, G. A., Headley, T. J., and Romig, Jr., A. D. 1986. The use of new PHACOMP in understanding the solidification microstructure of nickel base alloy weld metal. *Metallurgical Transactions* 17A(12): 2107-2115.

10. Ernst, S. C. 1991. Weldability studies of Haynes 230 alloy. *Welding Journal* 70(4): 80-s to 89-s.

11. Cieslack, M. J., Headley, T. J., Knorovsky, G. A., Romig, Jr., A. D., and Kollie, T. 1990. A comparison of the solidification behavior of INCOLOY 909 and INCONEL 718. *Metallurgical Transactions* 21A(2): 479-487.

12. Maguire, M. C., and Headley, T. J. 1990. A weldability study of Haynes Alloy 242. *Weldability of Materials: Proceedings of the Materials Weldability Symposium*, 167-173. Materials Park, Ohio: ASM International.

13. Knorovsky, G. A., Cieslack, M. J., Headley, T. J., Romig, Jr., A. D., and Hammetter, W. F. 1989. Inconel 718: A solidification diagram. *Metallurgical Transactions* 20A(10): 2149-2157.

14. Lundin, C. D., Liu, W., Zhou, G., and Qiao, C. Y. 1998. Unmixed zone in arc welds: Significance on corrosion resistance of high molybdenum stainless steels. Welding Research Council, *Bulletin* No. 428.

Preparation of Manuscripts for Submission to the *Welding Journal* Research Supplement

All authors should address themselves to the following questions when writing papers for submission to the *Welding Journal* Research Supplement:

- ◆ Why was the work done?
- ◆ What was done?
- ◆ What was found?
- ◆ What is the significance of your results?
- ◆ What are your most important conclusions?

With those questions in mind, most authors can logically organize their material along the following lines, using suitable headings and subheadings to divide the paper.

1) **Abstract.** A concise summary of the major elements of the presentation, not exceeding 200 words, to help the reader decide if the information is for him or her.

2) **Introduction.** A short statement giving relevant background, purpose, and scope to help orient the reader. Do not duplicate the abstract.

3) **Experimental Procedure, Materials, Equipment.**

4) **Results, Discussion.** The facts or data obtained and their evaluation.

5) **Conclusion.** An evaluation and interpretation of your results. Most often, this is what the readers remember.

6) Acknowledgment, References and Appendix.

Keep in mind that proper use of terms, abbreviations, and symbols are important considerations in processing a manuscript for publication. For welding terminology, the *Welding Journal* adheres to AWS A3.0:2001, *Standard Welding Terms and Definitions*.

Papers submitted for consideration in the *Welding Research Supplement* are required to undergo Peer Review before acceptance for publication. Submit an original and one copy (double-spaced, with 1-in. margins on 8 ½ x 11-in. or A4 paper) of the manuscript. A manuscript submission form should accompany the manuscript.

Tables and figures should be separate from the manuscript copy and only high-quality figures will be published. Figures should be original line art or glossy photos. Special instructions are required if figures are submitted by electronic means. To receive complete instructions and the manuscript submission form, please contact the Peer Review Coordinator, Doreen Kubish, at (305) 443-9353, ext. 275; FAX 305-443-7404; or write to the American Welding Society, 550 NW LeJeune Rd., Miami, FL 33126.